Considerations on protein stability during freezing and its impact on the freeze-drying cycle: a design space approach

ABSTRACT

Freezing is widely used during the manufacturing process of protein-based therapeutics, but it may result in undesired loss of biological activity. Many variables come into play during freezing that could adversely affect protein stability, creating a complex landscape of interrelated effects. The current approach to the selection of freezing conditions is however non-systematic, resulting in poor process control. Here we show how mathematical models, and a design space approach, can guide the selection of the optimal freezing protocol, focusing on protein stability. Two opposite scenarios are identified, suggesting that the ice-water interface is the dominant cause of denaturation for proteins with high bulk stability, while the duration of the freezing process itself is the key parameter to be controlled for proteins that are susceptible to cold denaturation. Experimental data for lactate dehydrogenase and myoglobin as model proteins support the model results, with a slow freezing rate being optimal for lactate dehydrogenase and the opposite being true for myoglobin. A possible application of the calculated design space to the freezing and freeze drying of biopharmaceuticals is finally described, and some considerations on process efficiency are discussed as well.

Keywords: proteins; protein aggregation; freeze-drying; Quality by design (QbD)

Abbreviations: CNTF: ciliary neurotropic factor, GDH: glutamate dehydrogenase, IL-1ra: interleukin-1-receptor antagonist, LDH: lactate dehydrogenase, Mb: myoglobin, OD: optical density, PFK: phosphofructokinase, QbD: quality by design, TNFbp: tumor necrosis factor binding protein

INTRODUCTION

The market of protein-based therapeutics has increased steadily in the last few years[1], but their intrinsic instability represents a critical issue. The biological activity of proteins is strongly related to their 3D conformation, which may be easily lost upon exposure to high/low temperature, presence of interfaces, pH shifts etc.[2]

Protein-based drugs or reference standards are often stored under frozen conditions to increase their stability and avoid physical, chemical or biological degradation. However, freezing could result in undesired loss of therapeutic potency. First, cold denaturation may occur at the low temperature used during freezing. The cold denaturation process is driven by the reduced penalty for water-hydrophobic interaction at low temperature, that promotes the exposure of the protein hydrophobic core to the solvent[3-7]. The crystallization

of water, with the formation of an ice-water interface, may also be harmful to protein stability, as proteins may denature while adsorbed onto the interface[8].

Furthermore, solutes concentration rapidly increases when ice is formed, and this may translate into significant changes in ionic strength and composition of the amorphous phase[9]. Because of this, it was even suggested that the rate of chemical reactions may actually increase when freezing an aqueous solution[10]. Some buffering species may also undergo selective crystallization, resulting in not negligible pH changes[11-14].

Finally, phase separation of polymers[15] or the crystallization of other formulation components[9,16] may lead to the formation of additional interfaces where the protein may adsorb and denature. As a consequence of phase separation, the protein may also preferentially partition into a phase where the concentration of protectants is too small to allow effective stabilization. It is therefore clear that a number of complex and strongly related phenomena come into play during freezing of a typical pharmaceutical solution, making the choice of the optimal process conditions not trivial.

As an example, the cooling rate is a variable that should be strictly controlled during freezing, as a faster cooling rate results in smaller ice crystals, and therefore larger ice-water interface[17,18]. A faster cooling rate may also help to prevent crystallization of buffering species, thus minimizing pH changes during freezing[19,20], and could affect the extent of crystallization of excipients, the polymorphs compositions changes during the lyophilization process, or the final polymorphs compositions[21-25]. The extension of the ice-water surface is also strongly influenced by the nucleation temperature, with a higher nucleation temperature resulting in larger crystals[26]. The thawing rate may also be crucial, as slow thawing promotes the recrystallization process, where small ice crystals grow into larger ones. Recrystallization results in undesired interfacial or shear stress for proteins at the ice-water interface, which may affect their activity.[27]

Freezing also constitutes the first step of the freeze drying, or lyophilization, process, which is widely used to increase the shelf life of many pharmaceutical products. Freeze drying allows removal of water at low temperature and is, therefore, particularly indicated for products that are sensitive to high temperature. During lyophilization, a product is first frozen by decreasing the temperature to low enough values (typically 233 / 223 K), and water is then removed at low pressure by sublimation (primary drying) and desorption (secondary drying).

During freeze-drying, the freezing protocol not only affects the protein stability, as previously discussed, but is also strictly related to the process efficiency. The pore size within the dried cake corresponds to the

size of ice crystals which are formed during freezing, provided that neither shrinkage nor collapse of the cake occurs. In turn, the pore dimension is intimately tied to the process efficiency and product quality. A large pore size promotes the removal of water by sublimation, decreasing the primary drying time[26], and results in a lower temperature within the product being dried, minimizing the risks of collapse. However, a small extension of the ice-water interface is also associated with reduced desorption rate, and therefore slower secondary drying[28].

Hence, the picture of interrelated effects on protein stability during freezing as outlined previously becomes even more complex when considering freeze-drying process duration and efficiency.

Despite the complexity of the subject, the selection of the freezing conditions is currently non-systematic, and this is not in line with the guidelines issued by regulatory agencies, that emphasize the necessity for a Quality by Design (QbD) approach[29]. QbD prioritizes process understanding and control in order to guarantee the desired characteristics of the final product[30-31].

In order to cover this gap, here we will demonstrate how the design of the freezing step of a freeze-drying cycle could benefit from the QbD concept. In particular, a design space approach will be used. Design space is a tool that may be used in the QbD process to provide useful information about the effect of input variables on output critical parameters. Here, the effect of cooling rate and nucleation temperature on protein stability will be investigated using this tool, and two opposite scenarios will be hypothesized, depending on the relative stability of proteins in bulk or at interfaces. In the first one, the ice-water interface is identified as the dominant cause of denaturation for proteins with high bulk stability, while in the second case the duration of the freezing process itself is suggested to be the key parameter for those proteins that are highly sensitive to cold denaturation. The results of experimental tests on lactate dehydrogenase (LDH) at pH 6.5 and myoglobin (Mb) at pH 3.7 will be reported, that support the model results. Finally, in the framework of the freeze drying of biopharmaceuticals, some considerations on process performance will also be given, together with some guidance on the relevance of the model scenarios for commonly used biotherapeutics. While the complexity of the phenomena involved in the freezing of a protein formulation can hardly be fully described by a mechanistic model, the proposed approach still aims to provide some useful indications. To the best of our knowledge, this is the first attempt to describe protein stability during freezing using a fully mechanistic approach. In this work, general considerations on protein stability will be extracted from this model, so as to make the discussion as general as possible. These indications may help to guide professionals into the selection of appropriate freezing conditions, which are beneficial for the preservation of

protein biological activity, and to ensure process economic efficiency at the same time. For this work we will focus on small scale freezing (i.e., freezing in small volumes, such as vials). The complications created by the larger heat and mass transfer dimensions of large-scale systems will therefore not be addressed.[32]

MATERIALS AND METHODS

Simulation Approach

Freezing of a protein-based active ingredient was considered in this work, and a two-state unfolding process of a protein, from the native (N) to denatured (U) state, was hypothesized. A two-state kinetic model is valid if the following assumptions are met: (i) a single folded state, and a large number of unfolded states can be identified; (ii) each unfolded state gives a small contribution to the total partition function of unfolded states; (iii) transition rate constants are inversely proportional to the partition functions of single conformational states, and each unfolded state can transition to several other unfolded states; (iv) the boundary factors in transition rate constants are not influenced by changes in folding conditions; (v) there are no large barriers between unfolded states which could result in the protein being trapped for a long time[33,34].

In a two-state process, the mole fraction of unfolded protein, at thermodynamic equilibrium, is given by,

$$f_U = \frac{[U]}{[N] + [U]} = \frac{K}{1 + K} \tag{1}$$

where the equilibrium constant K depends on the free energy of unfolding ΔG,

$$K = e^{-\Delta G/RT} \tag{2}$$

R is the universal gas constant, and T the absolute temperature.

The free energy change depends on temperature and concentration c of an excipient according to,

$$\Delta G(T, c) = \Delta H_0 - T\Delta S_0 + \Delta C_p[T - T_0 - T \ln T/T_0] + mc \tag{3}$$

ΔH_0, ΔS_0 and ΔC_p are the enthalpy, entropy and specific heat change upon unfolding at a reference temperature T_0. The proportional coefficient m depends on the particular excipient considered.

In most cases, the thermodynamic equilibrium is not reached during the freezing process, and a kinetic approach should be used. For a reversible two-step process, it is possible to write the following system of differential equations

$$\begin{aligned}\frac{d[U]}{dt} &= -k_f[U] + k_u[N] \\ \frac{d[N]}{dt} &= +k_f[U] - k_u[N]\end{aligned} \tag{4}$$

where the kinetic constants k_f and k_u depend on temperature, osmolyte concentration and solution viscosity μ[35,36]. Moreover, we can assume the unfolding process as an activated process, characterized by the presence of a transition state TS,

$$\begin{aligned}k_u(T,\, c,\, \mu) &= A\frac{\mu_0}{\mu}e^{-\Delta G^{N-TS}/RT} \\ k_f(T,\, c,\, \mu) &= A\frac{\mu_0}{\mu}e^{-\Delta G^{U-TS}/RT}\end{aligned} \tag{5}$$

A is a constant for any protein, and μ_0 the viscosity at some reference conditions (293 K, 1 bar and pure water in our case, i.e., μ_0 = 1cP). In practice, we describe the conformational dynamics of proteins in viscous solutions using a version of the Kramers' theory[37,38,39] where the contribution given by the internal friction of the protein has been considered negligible[36]. This assumption is particularly justified in the case of a freezing process, where the solvent friction should dominate because of the large values of viscosity that are eventually reached. The free energy change associated to the passage from native or denatured state, and the transition state TS, is given by

$$\Delta G^{X-TS}(T,\, c) = \Delta H_0^{X-TS} - T\Delta S_0^{X-TS} + \Delta C_p^{X-TS}[T - T_0 - T\ln T/T_0] + m^{X-TS}c \tag{6}$$

with X=N, U. In a two-state process, we also have that $\Delta G = \Delta G^{N\text{-}TS} - \Delta G^{U\text{-}TS}$.

In the present work, realistic values were chosen for all the parameters related to protein stability, but with no reference to any specific protein. These values were also varied among different simulations, to cover an as wide as possible range of protein folding stabilities. The results presented in the following aim, therefore,

to have general validity, qualitatively describing a variety of situations that may occur during the freezing of a protein formulation.

First of all, the ice crystal size dimension was calculated using a mechanistic model[40], with the iterative procedure described in [41]. A typical pharmaceutical process, where a protein formulation is filled into vials and loaded onto the shelves of a freeze dryer, was considered during the simulations. Freezing of a 5% w/w sucrose formulation with a 150:1 sucrose to protein mole ratio was considered. During the simulations, the shelf temperature T_{shelf} was linearly decreased from 293 to 233 K, with varying cooling rates over the range 0.1-1 K min^{-1}. The nucleation temperature was also varied in the range 248-265 K, and an 8x8 matrix of cooling rate x nucleation temperature conditions was considered to build the design space, as it was done in [42]. The average ice crystal size d_p within the product was computed for each point of this matrix, and the resulting ice-water surface area S was computed from,

$$S = \frac{4m_w}{d_p \rho} \tag{7}$$

where ρ is the ice density, m_w the initial mass of water in the vial, and the assumption was made that ice crystals are cylinder-shaped.

The increase in sucrose concentration as a result of the freezing process was computed using the data reported in [43]. The solution viscosity as function of temperature and excipient concentration was then calculated using the scaled Arrhenius equation,

$$\log_{10} \frac{\mu}{\mu_0} = a + b \left(\frac{T_g}{T}\right) + c \left(\frac{T_g}{T}\right)^2 \tag{8}$$

where T_g is the glass transition temperature, and the coefficients a, b and c were taken from [44].

For the estimation of ΔG, values of 0.2 kJ kmol^{-1} K^{-1}, 3 kJ kmol^{-1} K^{-1} and 295 K were considered for ΔS_0, ΔC_p and T_0, respectively. These values were chosen because are in the range often encountered for proteins. For instance, similar parameters were measured for protein L in a previous work[35]. By contrast, the values of ΔH_0 and m were varied from simulation to simulation, to sample different situations of protein bulk stability. The kinetic constants k_u and k_f were then computed assuming $\Delta G^{N\text{-}TS} = 1.5\ \Delta G$ and $\Delta G^{U\text{-}TS} = 0.5\ \Delta G$,

while the constant A in Eq. (5) was again changed from simulation to simulation. The ratio 3:1 for $\Delta G^{N\text{-}TS}/\Delta G^{U\text{-}TS}$ has been chosen arbitrarily, because not many data on the temperature dependence of folding kinetics are currently available in the literature.

Equations 4 were then solved in Matlab R2017a, using a 0.1 s time-step. The percentage of unfolded protein as a result of bulk denaturation could therefore be computed. However, surface-induced denaturation may also occur, as a result of adsorption to the ice-water interface. From equation 7 it was possible to calculate the final extension S of the ice-water surface interface, while its change during the process was estimated from

$$S_i(t) = S\,\frac{c_{w,end}}{c_w(t)} \tag{9}$$

where $c_{w,end}$ is the water mass fraction at the end of freezing, while c_w represents its current value.

The percentage of surface-denatured molecules was finally computed assuming that the protein behavior was perturbed whenever it was closer than d_i=4 nm to the ice surface. This threshold was chosen because a long-ranged effect of the ice surface, up to 4 nm from the interface, was observed in molecular dynamics simulations of the GB1 peptide[45], and preliminary data for another model protein (unpublished data) confirm this observation. To determine the number n_p of adsorbed protein molecules (having molar mass M_p and molecular volume V_p), the following system of equations was solved,

$$\begin{aligned} n_w M_w &= c_w(n_w M_w + n_p M_p + n_s M_s) \\ S_i d_i &= V_w n_w + V_p n_p + V_s n_s \end{aligned} \tag{10}$$

where n_s and n_w are the number of adsorbed sucrose and water molecules, respectively, while M_w, M_s and V_w, V_s are their molar masses and molecular volumes. It was assumed that the ratio n_s/n_p was the same as in the bulk, i.e., 150. It was also assumed that the surface-driven denaturation of the protein occurred with no thermodynamic barrier. This means that 50% of the adsorbed protein molecules are in the unfolded state.

For the simulations, both the completely reversible situation, and the completely irreversible one, were considered. In the latter case, Equations 4 were modified to,

$$\frac{d[U]}{dt} = k_u[N]$$
$$\frac{d[N]}{dt} = -k_u[N] \quad (11)$$

The irreversible situation corresponds, for instance, to the case of proteins that tend to form aggregates when they are in the unfolded state. In this case, the unfolded molecules that cluster to form an aggregate and precipitate cannot convert back to their native state anymore.

The parameters used for the simulations performed in this work are listed in Table 1. The simulated conditions were chosen so as to explore a wide range of protein bulk stability, from the point of view of both thermodynamics (different ΔH_0, see Figure 1, and different m), and kinetics (different pre-exponential factor A), while keeping fixed the behavior at the ice surface. In addition, considering the values of $\Delta G^{N\text{-}TS}$ and $\Delta G^{U\text{-}TS}$ selected for this work, the values of A listed in Table 1 made it possible to have denaturation kinetics compatible, i.e., neither too fast nor too slow, with the simulation timescale. Simulations 1 and 3 correspond to proteins that are significantly more stable in bulk solution than at the surface. By contrast, the model proteins described in simulations 2 and 4 are unstable in bulk and tend to unfold quickly at the low temperature experienced during freezing.

If the freezing constitutes the first step of a freeze drying process, some considerations on process efficiency could also be made. The crystal size d_p of the frozen product equals the pore dimension of the dried cake, provided that no collapse occurs. In turn, the pore dimension determines the mass transfer resistance to vapor flow during primary drying, and, therefore, primary drying time t_d and maximum temperature reached during this phase T_{max}. Thus, in order to assess the effect of ice crystal size on t_d and T_{max}, a simple 1-dimensional model was used[46]. The primary drying model was implemented in Matlab and solved using the finite differences approach, with a 60 s timestep.

It should be taken into account that the model here introduced cannot, at present, describe the thawing process, where protein unfolding may also occur. Therefore, the experiments described in the following section were all performed changing the freezing protocol only, while keeping fixed the thawing conditions. This made it possible to compare the effect of freezing on protein stability, and make a more direct comparison with the model results. The possible addition of thawing effects in the model will be the subject of future investigations.

Experimental Validation

Some experimental tests were performed to validate the simulation results. Myoglobin (Mb from equine heart, Sigma Aldrich, Milan, Italy) and lactate dehydrogenase (LDH from rabbit muscle, Sigma Aldrich, Milan, Italy) were selected as model proteins.

Freeze-Thaw Cycles on Myoglobin

Myoglobin was dissolved in 10 mM sodium citrate buffer at pH 3.7. Citrate buffer was selected because its pH remains constant during freeze-thawing experiments[20]. Mb concentration was adjusted to either 0.1 or 0.2 mg/ml, and the presence of the surfactant Tween 80 (Sigma Aldrich, Milan, Italy) at 0.01% w/v was also considered for this study. All the solutions were prepared using water for injection (Fresenius Kabi, Verona, Italy), and filtered using 0.2 μm filters.

To assess the effect of different ice-water surface areas on protein stability, three different freezing protocols were used. In the first one, samples were frozen by immersing vials (0.5 ml Screw Cap GeNunc Storage Vials, HDPE, Sterile, Thermo Fisher Scientific, Rochester, NY, USA) into liquid nitrogen for 5 min, and then thawed in air at room temperature.

In the second and third protocol, 2 ml of each sample were filled into 4R 16x45 mm vials (Nuova Ompi glass division, Stevanato Group, Piombino Dese, Italy), partially stoppered with silicon stoppers (West Pharmaceutical Services, Milan, Italy) and loaded onto the shelves of a freeze dryer. In one case, shelf-ramped freezing was performed at 1 K/min, from 283 to 238 K using a Revo (Millrock Technology, Kingston, NY, USA) freeze dryer. In the other case, the controlled nucleation technique known as vacuum induced surface freezing (VISF) was used.[47,48] This cycle was performed in a LyoBeta 25 (Telstar, Terrassa, Spain) freeze dryer, where the vials were first equilibrated at 268 K for 1 h. At that point, pressure inside the chamber was lowered to about 1 mbar. This promoted strong evaporation from the product surface, and therefore a reduction in temperature that induced nucleation in all the vials more or less at the same time (approximately in 30 s). Pressure was subsequently released to the atmospheric value, and the product equilibrated at 268 K for 1 h to promote the formation of big ice crystals. Finally, temperature was decreased to 238 K at 0.5 K/min. For both cycles, the cooling rate was also monitored by means of T-type miniature thermocouples placed inside some non-active (containing only the buffer) vials. In all cases, samples were thawed in air at room temperature.

In the case of quench cooling in liquid nitrogen, a large ice-water surface area should be formed, while the biggest ice crystals should be obtained by using the VISF protocol, where the high nucleation temperature (268 K) and the holding time at 268 K should promote the ice crystals growth. In the case of quench and shelf-ramped freezing, three freeze-thaw cycles were performed, and samples were analyzed both after the first and the third cycle. By contrast, only one freeze-thaw cycle was performed using the VISF technique. After thawing, the protein solutions were centrifuged at 13000 rpm for 5 min (Heraeus Megafuge 8 Centrifuge Series, Thermo Fisher Scientific, Milano, Italy), and the percentage of aggregates was thereafter calculated from the decrease in protein concentration (UV detection at 280 and 410 nm) after centrifugation. Optical density (OD) was measured against a solvent-matched reference using a 6850 UV/VIS spectrophotometer (Jenway, Stone, Staffordshire, UK). This analysis cannot provide detailed information about the secondary and tertiary structure, or biological activity, of Mb in solution; however, it allowed us to indirectly measure protein denaturation and the presence of large precipitates, which is enough for the purpose of this study. The peak centered at 280 nm in the Mb absorbance spectrum is due to aromatic amino acids (primarily tryptophan and tyrosine) in the polypeptide and to the heme iron, and its location is characteristic of most proteins. The other absorption peak centered at approximately 410 nm is due entirely to the heme and is commonly referred to as the Soret band[49].

The presence of stabilizing additives was also considered, and a freeze-thaw cycle was therefore performed on 0.1 mg/ml myoglobin in 5% w/w sucrose, 5% w/w trehalose, or 5% w/w mannitol, again using the Revo freeze dryer (Millrock Technology, Kingston, NY, USA). All the formulations were prepared in 10 mM sodium citrate buffer at pH 3.7, and a 0.1 mg/ml myoglobin solution in buffer only (without cryo- or lyoprotectants) was also considered. The formulations were prepared both with and without 0.01% w/v Tween 80, to investigate the effect of surfactants.

Freezing was performed using a 1 K/min cooling rate, and the protein recovery was measured by UV/VIS spectroscopy at 410 nm after thawing in air at room temperature, using a spectrophotometric multiwell plate reader (Multiskan FC Microplate Photometer, Thermo Fisher Scientific, Milano, Italy).

Freeze-Thaw Cycles on Lactate Dehydrogenase

LDH was dialyzed against 10 mM sodium citrate buffer at pH 6.5. Dialysis was performed at 277 K, and the buffer was changed 3 times (the first 2 times every 3 h, while the third dialysis step was carried out

overnight). The concentration of LDH after dialysis was determined using UV/VIS spectroscopy (6850 UV/VIS Spectrophotometer; Jenway, Stone, Staffordshire, UK). The peak at 280 nm was monitored, and an extinction coefficient of 1.44 mL/(mg cm) was used for calculations.

Two different freeze-thaw protocols were tested on 0.1 mg/ml LDH in 10 mM sodium citrate buffer at pH 6.5, 5% w/w sucrose, 5% w/w trehalose, or 5% w/w mannitol. All the formulations were prepared in 10 mM sodium citrate buffer at pH 6.5, both with and without 0.01% w/v Tween 80, and filtered using 0.2 μm filters. The first protocol was quenching in liquid nitrogen, while the second one consisted in shelf-ramped freezing at 1 K/min cooling rate. The same approach previously described for Mb was used for both protocols. After thawing in air at room temperature, the enzymatic activity of LDH after 1 freeze-thaw cycle was calculated from the increase in absorbance at 450 nm due to the reduction of NAD to NADH. A standard curve built with 1.25 mM NADH standard was used to calculate the amount of NADH generated in each well. For this analysis, 0.2 mg/ml LDH in 10 mM sodium citrate buffer at pH 6.5, with or without 0.01% w/v Tween 80, was also considered. The degree of aggregation in each sample was also measured from the increase in absorbance at 500 nm, which is a measure of turbidity. However, this last analysis was performed after 9 freeze-thaw cycles, so as to increase the strength of the signal. In all cases, a spectrophotometric multiwell plate reader (Multiskan FC Microplate Photometer, Thermo Fisher Scientific, Milano, Italy) was used for the analyses.

Low-Temperature Storage

Mb and LDH were selected as model proteins because they are characterized by very different cold denaturation temperatures (283 K for Mb at pH 3.7 according to [50] and 245 K for LDH at neutral pH[51]). To further confirm their different behavior at low temperature, 0.1 mg/ml Mb in 10 mM sodium citrate buffer at pH 3.7 and 0.1 mg/ml LDH in 10 mM sodium citrate buffer at pH 6.5 were kept for 24 h at 268 K, where no freezing was observed. The presence of 0.01 % w/v Tween 80 was also considered. Protein stability over this time was monitored from the decrease in absorbance at 410 nm, in the case of Mb, or the ability to reduce NAD to NADH, in the case of LDH, as previously described.

RESULTS AND DISCUSSION

An Insight Into Protein Behavior during Freezing

The behavior of a model protein during freezing has been simulated. A typical output of a simulation is shown in Figure 2. Before the nucleation event, the solution viscosity μ is too low to significantly hinder the conformational changes of the protein, and the kinetic constants show moderately high values. Immediately after the nucleation event, i.e., after 0.7 h in the case of Figure 2, the excipient concentration c increases sharply because of the formation of ice crystals (Figure 2a), and this augments the bulk stability of the protein. This is evident from Figure 2b, where the free energy change ΔG is shown both including (red curve) or neglecting (black curve) the effect of the osmolyte. In this case, the effect of the excipient is stabilizing (positive m-value), as it shifts the free energy of unfolding to larger values. While the two curves are almost superimposed before nucleation, they clearly split apart as soon as the first ice crystals are formed. The solution viscosity increases as well (Figure 2a), kinetically hindering any protein movement. As a consequence, the kinetic constants k_u and k_f drop to very low values (Figure 2d). Surface-driven denaturation becomes therefore dominant after nucleation, and a not negligible amount of protein molecules adsorbs to the ice surface (Figure 2c), potentially undergoing conformational changes.

The resulting fraction of unfolded (U) and native (N) protein molecules as function of freezing time is shown in Figure 3. In the case of Figure 3a, simulation 1 in Table 1 is considered. In this case, the protein is stable in bulk, as the folding rate constant (k_f) is remarkably larger than the unfolding (k_u) one (see Figure 2d). Therefore, the protein molecules that unfold almost immediately convert back to the native state, and no notable unfolding occurs before nucleation. Once nucleation occurs, surface-driven denaturation prevails and, as observed in Figure 3a, the amount of unfolded proteins suddenly increases.

On the other hand, if the same values of ΔH_0, m and A are used, but an irreversible process (simulation 4 in Table 1) is considered (Figure 3b), a significant percentage of the protein undergoes conformational changes before nucleation, and the denaturation that is subsequently induced by the ice surface plays only a secondary role. As evident from this first example, a major contribution is therefore played by the ratio between bulk and surface stability. A design space approach was therefore used to further investigate the implications of this observation.

The Design Space Suggests the Existence of Two Opposite Behaviors

The objective here is to identify the parameters that may be responsible for an increased loss of therapeutic activity during the freezing step of freeze drying, and should therefore be monitored during the process. As we are not interested in the absolute value of unfolded protein molecules in each configuration, the graphs

will show the percentage of unfolded molecules (U), normalized by the maximum value observed in each design space (U_{max}). This will allow an easier comparison between different simulations.

In line with previous considerations, the design space for simulation 1 (Figure 4a) shows that the worst condition for protein stability (U/U_{max} = 100%) corresponds to the region of high cooling rates and low nucleation temperature. As mentioned in the Introduction, small ice crystals are formed in these conditions, that result in a large ice-water surface, as shown by the red isocurves in Figure 4. It is evident that the greater the extension of the ice interface is, the more the protein unfolds. In these conditions surface-induced denaturation prevails, and the optimal process should maximize the ice crystal size. This may be achieved using a low cooling rate or inducing nucleation at high temperature by means of a controlled nucleation approach[52], as the VISF protocol employed in this work. Alternatively, the use of surfactants should be considered to minimize protein-surface interactions[53]. Because of their amphiphilic nature, surfactants preferentially locate at interfaces, thus reducing adsorption phenomena, and therefore also surface-induced denaturation.[45,54]

If the protein has a reduced stability in bulk, as in simulation 2, surface-induced denaturation becomes less important. In this case (Figure 4b), a low cooling rate results in the highest degree of protein unfolding. This happens because the lower the cooling rate is, the longer the solution viscosity is low enough to allow fast conformational changes. Therefore, if a protein with low bulk stability is considered, a high cooling rate may be beneficial, as it would result in shorter freezing times and earlier cryo-concentration.

Similar considerations apply to the case of irreversible conformational changes. In the case of simulation 3 (Figure 4c), surface-driven unfolding is again dominant and slow cooling rates/high nucleation temperature conditions should be preferred. On the other hand, if the denaturation process in the bulk solution is thermodynamically and kinetically favored, as in simulation 4 (Figure 4d), the extension of the ice interface is not a crucial parameter, while the duration of the freezing process should be strictly controlled, and a cryo-concentrated matrix should be formed as quickly as possible. Overall, Figure 4 shows that surface-induced unfolding is dominant in simulations 1 and 3 in Table 1, while it becomes less important in the case of simulations 2 and 4.

Finally, the effect of protein concentration has been investigated in Figure 5. In this case, a fixed value of 263 K was chosen for the nucleation temperature, and the cooling rate was again varied from 0.1 to 1 K/min. Conditions 3 and 4 in Table 1 were considered, and the protein concentration was varied between 0.001 and 0.01 mol/l. In the case of proteins having high bulk stability (conditions 3 in Table 1, Figure 5a), surface-

driven denaturation is dominant, and increasing the protein concentration has a significant positive effect. This occurs because the extension of the ice-water interface is finite, and the number of protein molecules adsorbed at the surface cannot exceed a given value. When this value is reached, increasing the bulk concentration reduces the percentage of unfolded molecules.

By contrast, the effect of protein concentration is not equally important when cold denaturation in the bulk is the dominant mechanism (conditions 4 in Table 1, Figure 5b). In this case, only a very slight increase in protein recovery is observed when moving from 0.001 to 0.01 mol/l, and is again related to the smaller percentage of protein molecules adsorbed at the ice surface at higher concentration.

It should be pointed out that the contour plots shown in Figures 4 and 5 were computed for reference values of protein thermodynamics and kinetics parameters (ΔH_0, ΔS_0, ΔC_p, *m, A* etc.) and the relative trends only were here discussed. Considering that this is the first attempt to include protein stability in a design space approach, this was done with the aim to make the discussion as general as possible. It would anyway be possible to use this same modeling approach to obtain specific information for the protein being considered, by specifically adjusting the folding parameters included in the model.

Comparison with Experimental Data

For experiments, different freezing protocols were selected, that correspond to either the far left (slow process) or far right (faster process) of Figure 4. A very fast freezing protocol, i.e., quench cooling in liquid nitrogen, was also used as an extreme representative of a fast freezing process, with the objective to enhance the observed effects on protein stability. The behavior of proteins during freezing is extremely complicated, and several factors should in principle be considered. However, two possible scenarios were investigated and described by the simple model presented in this work. The first one, that primarily ascribes protein denaturation to adsorption at the ice-water interface, was confirmed in the case of LDH as model protein (see Figure 6). In panel (a), the recovery of protein enzymatic activity after 1 freeze-thaw cycle is shown, as measured from the increase in OD at 450 nm due to the reduction of NAD to NADH. In panel (b), the increase in OD at 500 nm due to aggregation after 9 freeze-thaw cycles has been considered to estimate protein recovery. Both quench freezing and shelf-ramped freezing at 1 K/min were considered. Plastic vials were used for the quench freezing protocol for their better compatibility with the available equipment. However, preliminary tests for 0.1 mg/ml LDH in 10 mM sodium citrate buffer at pH 6.5 or 0.1 mg/ml

myoglobin in 10 mM sodium citrate buffer at pH 3.7, with or without 0.01% w/v Tween 80, were used to verify that no significant difference existed with the results obtained in 4R 16x45 mm glass vials.

It is evident that the quench freezing in liquid nitrogen (blue bars) resulted in reduced protein recovery compared to the shelf-ramped freezing at 1 K min^{-1} (grey bars). The formation of extremely small ice crystals, and therefore of a huge ice-water surface area, during quench freezing may be at the basis of this observation.

In all cases, the addition of 0.01 % w/v Tween 80 remarkably reduced protein aggregation, as evident from Figure 6b, and often resulted also in increased protein activity, as shown in Figure 6a. More specifically, the addition of surfactant always led to improved recovery of LDH activity when quench freezing was performed (blue bars in Figure 6a). This further suggests that surface-driven denaturation was dominant, especially for the case of the quench freezing protocol. Sucrose and trehalose at 5% w/w resulted in improved protein activity (Figure 6a), even though they did not remarkably decrease protein aggregation at 1 K/min cooling rate (Figure 6b). By contrast, the addition of the crystalline excipient mannitol, in absence of surfactants, was deleterious for protein aggregation at this cooling rate, as it resulted in increased turbidity of the solution after freeze-thawing. This increase in aggregation may be related to the formation of mannitol crystals at 1 K/min, where the protein may adsorb and denature. This explanation is also supported by the fact that when Tween 80 was added to the mannitol formulation, the protein recovery significantly increased, as regards both enzymatic activity (Figure 6a) and aggregation (Figure 6b). However, the quench frozen samples containing cryoprotectants, and in absence of surfactants, all showed an increase in protein recovery compared to the buffer only formulation, and behaved very similarly, suggesting that mannitol did not crystallize under these conditions, in line with previous observations.[24,25] This effect of cryoprotectants and surfactants was not explicitly discussed in the simulation part of this work, but could be included in the model by modifying the value of *m* in Equations 3 and 6, or the adsorption behavior at the ice interface (in the case of surfactants, Equations 10). Finally, the recovery of LDH enzymatic activity was also tested for a different concentration, 0.2 mg/ml in Figure 6a. For both shelf-ramped freezing and quench freezing, protein recovery improved when moving from 0.1 to 0.2 mg/ml. As shown in Figure 5a, this beneficial effect observed upon increasing the protein concentration is not surprising when surface-driven denaturation is dominant.

The behavior discussed in this work for LDH is also well-documented in the literature. For instance, using LDH as model protein, a remarkable loss of activity was observed in frozen systems, while no degradation

was detected in concentrated solutions at the same temperature and composition, but without ice[55]. Similarly, solutions of the azurin protein exhibited a dramatic decrease in the average phosphorescence lifetime of the Trp-48 residue at the onset of ice formation, which is indicative of protein unfolding[8]. Moreover, phosphofructokinase (PFK), lactate dehydrogenase (LDH), glutamate dehydrogenase (GDH), interleukin-1-receptor antagonist (IL-1ra), tumor necrosis factor binding protein (TNFbp), and ciliary neurotropic factor (CNTF) were observed to form a large amount of insoluble precipitates when quench cooled in liquid nitrogen, while a smaller cooling rate caused significant less precipitation[56]. Also, the addition of a small amount of surfactant could effectively prevent the observed precipitation. These results suggest that surface-driven denaturation at the ice-water interface is dominant for many proteins and indicate that the behavior described in Figures 4a and 4c is commonly observed in experiments.

On the contrary, it is more difficult to find in the literature reports of proteins that behave according to Figures 4b and 4d. This occurs because many of the proteins commonly used for this type of experiments show a quite high bulk stability and are unlikely to exhibit any significant denaturation before the onset of ice formation. In contrast, the model protein selected in this work, namely, myoglobin, is extremely sensitive to cold denaturation, especially at the low pH (3.7) selected for this study.[50,57] In Figure 7, the percentage of myoglobin recovery after freeze-thawing is shown, as measured from the OD at 280 nm (Figure 7a) or 410 nm (Soret band, Figure 7b). The peak at 280 nm is related to protein concentration. Therefore, a decrease in the peak at 280 nm after freeze-thawing and centrifugation is indicative of aggregation. By contrast, while the peak at 410 nm shows a similar dependence on concentration, it may also be affected by changes in the conformation of Mb. For instance, it was observed that the disruption of the secondary and tertiary structure of Mb by addition of 8 M urea caused a decrease in the extinction coefficient at 410 nm, while no changes were observed for the peak at 280 nm[49]. This happens because the heme pocket modifies its conformation, and is exposed to a different environment, when Mb unfolds. The Soret band is altered whenever the physical environment of the heme changes, and therefore represents a useful indicator of the protein conformation. The different significance of the OD values at 280 nm (aggregation) and 410 nm (aggregation + denaturation) also accounts for the lower values of protein recovery generally reported in Figure 7b than in Figure 7a. Some denatured protein molecules may still be in the monomeric form, contributing to an increase in the peak at 280 nm, while not being detected at 410 nm.

As can be observed from Figures 7a and 7b, the VISF protocol (black bars) resulted in the worst protein recovery, while quench cooling in liquid nitrogen (orange bars) generally preserved activity the most, and

shelf-ramped freezing at 1 K/min (blue bars) showed an intermediate behavior. Overall, this indicates that surface-driven denaturation is not the main source of stress for the protein. In fact, the freezing protocol resulting in the largest ice-water surface area, i.e., quench freezing, led to an increase in protein recovery. By contrast, the data are compatible with bulk denaturation being the controlling mechanism. In this case, the time spent by the protein in a liquid solution at low temperature, where cold unfolding may ensue, should be minimized. The VISF protocol includes two holding steps at low temperature (268 K) and low solution viscosity (liquid or still not completely frozen matrix), that may promote the conformational changes responsible for aggregation and denaturation. The formation of a cryoconcentrated matrix occurs more quickly in the case of shelf-ramped freezing and is extremely fast when vials are directly immersed into liquid nitrogen. These results indicate that also the second scenario identified by the simulations, and illustrated in Figures 4b and 4d, can be experimentally observed, and this suggests that the simulation approach can capture at least the main features of protein stability during freezing.

The dominant role of bulk denaturation for myoglobin at pH 3.7 is also evident from the observed effect of surfactants. When surface-driven unfolding is the main mechanism, addition of polysorbates results in significantly increased protein stability.[54,56,58,59] However, addition of Tween 80 led to a reduced recovery of protein activity in our freeze-thaw experiments, as particularly evident from the absorbance values at 410 nm (Figure 7b). One possible explanation would be that surfactants have an effect on the conformation of myoglobin at low pH. This is an interesting observation, especially considering that the literature is controversial on this point. For instance, while some authors suggested that the polysorbates may have an effect on the secondary structure of a protein in the bulk[60,61], others theorized that this effect was negligible[62,63]. The disagreement on this point also arises from the close interrelation of surface-driven phenomena and bulk effects that generally occurs when dealing with a protein formulation. Thanks to our modelling approach, a situation was identified where these two effects can be more easily separated, making it possible to isolate the effect of surfactants in the bulk solution.

Finally, it is interesting that doubling the Mb concentration, from 0.1 to 0.2 mg/ml, generally increased protein recovery. According to our simulations (Figure 5), an increase in concentration should reduce the percentage of protein molecules adsorbed onto the ice-water surface area and remarkably affect stability when surface-driven denaturation is prevailing (Figure 5a). However, a smaller effect should be observed when bulk unfolding is the controlling mechanism (Figure 5b). We may therefore hypothesize that, even though the controlling mechanism of Mb aggregation and unfolding at pH 3.7 is related to cold denaturation,

adsorption onto the ice surface still plays a role, that translates into the observed improvement in protein recovery at higher concentration. This hypothesis is also supported by the smaller difference observed for the two values of protein concentration upon addition of Tween 80 (Figure 7). Even though Tween 80, as previously discussed, has a denaturing effect in the bulk, it still preferentially locates at interfaces, preventing adsorption. Therefore, if minimization of surface effects is the mechanism, the improvement related to an increase in protein concentration should become negligible in presence of surfactants. The observed stabilization may, however, also be related to the formation of more stable multimers, or by volume exclusion effects that arise at higher concentration. This last explanation was also proposed in a previous work[64], where the cold denaturation temperature of β-lactoglobulin was found to decrease significantly when increasing the protein concentration.

The effect of the addition of protectants such as sucrose, mannitol and trehalose, was also investigated (see Figure 8), both in presence (grey bars) and absence (dashed bars) of Tween 80. Data have been normalized relative to the formulation before freeze-thaw. It is apparent that the addition of excipients improved the recovery of protein activity after freeze-thawing, and this effect was particularly remarkable in presence of Tween 80. This is in line with the stabilizing effect of sugars on cold denaturation observed in previous works.[64] It is also particularly interesting that when either sucrose or trehalose was present, addition of the surfactant was not deleterious. We may hypothesize that these two amorphous excipients can effectively counteract the denaturing effect of Tween 80. As for the crystalline excipient considered in this work, i.e. mannitol, it behaved similarly to the disaccharides sucrose and trehalose in absence of surfactant. This once more suggests that surface-driven denaturation is not the main mechanism of protein denaturation for myoglobin at pH 3.7, as in this case crystallization of mannitol would create another surface onto which adsorption and unfolding may occur. However, the fraction of mannitol that remains in the amorphous phase together with the protein is probably not as effective as sucrose and trehalose in counteracting the denaturing effect of Tween 80. In fact, upon addition of the surfactant to the mannitol-based formulation, a decrease in protein recovery is observed, similarly to what occurs in citrate buffer only.

To further confirm the results obtained for Mb and LDH, their stability during a 24 h storage at 268 K was monitored, as shown in Figure 9. No freezing was observed in this case, and cold denaturation could therefore be the only possible explanation for a potential decrease in protein recovery. Such decrease was not observed in the case of LDH (dashed lines in Figure 9) over the time considered, and the protein activity was almost completely recovered after 24 h, both in presence and absence of Tween 80. This suggests that

the decrease in LDH activity observed during the freeze-thaw cycles was mostly related to the formation of the ice-water interface, in line with previous considerations.[55] Tween 80 did not remarkably affect LDH stability during storage at low temperature, and its positive effect during the freezing experiments presented in Figure 6 should therefore be mostly related to inhibition of protein interaction with the ice surface.

The situation was reversed in the case of Mb as model protein (solid lines). In this case, a significant loss in protein recovery was observed already after 1 h storage at 268 K, and only 64 % or 56 % protein activity were eventually recovered after 24 h, in absence or presence of Tween 80, respectively. These results confirm that Mb is unstable in a bulk solution at low temperature, and that its denaturation occurs quickly, thus explaining why fast immobilization of Mb in a frozen matrix during quench freezing is beneficial. The effect of Tween 80 is again observed to be detrimental for Mb stability, also during storage at low temperature.

Some Considerations on Process Performance and Suggestions for Process Development Scientists

In addition to protein stability, process efficiency should also be considered, if the product has to be freeze dried. As previously mentioned, the ice crystal size corresponds to the pore dimension that is formed within the dried product, provided that no collapse occurs. A large pore size reduces the resistance to mass transfer, and promotes the sublimation process, thus resulting in shorter drying times and lower product temperature, as schematized in Figure 10, where the primary drying time t_d and maximum product temperature T_{max} have been calculated as function of cooling rate and nucleation temperature, similarly to what was done in [42]. A fluid temperature and chamber pressure of 253 K and 10 Pa, respectively, have been considered for simulations of the primary drying step.

Overall, the hope of the authors is that this work may help formulation and process development scientists working with protein-based therapeutics. Proteins are often stored in the frozen or freeze-dried state, which is generally preferred over liquid storage because the solid state results in increased stability and shelf life.[65] To distinguish between the two scenarios here identified, i.e., controlling surface-induced or bulk degradation, a thermodynamic study may first be performed, with the objective to determine the enthalpy and entropy of protein unfolding/refolding. In this way, the temperature dependence of protein stability could be resolved[50]. Afterwards, the denaturation of a protein solution at low temperature, but in absence of ice, could be monitored to obtain some kinetic information, as shown in Figure 9. If no significant aggregation/loss of activity occurs during the typical timescale of a freezing process, as for LDH at pH 6.5 in

this work, then surface-induced denaturation may be dominant during freezing, and a slow freezing rate may be beneficial. Addition of surfactants in this case may help to further improve protein recovery, provided that the surfactant-protein interaction is not detrimental. On the other hand, if the protein being considered undergoes fast denaturation (i.e., faster than a typical freezing process) during the abovementioned experiment, as for Mb at pH 3.7 in this work, a fast cooling rate should be used, to entrap the protein in a solid matrix as quickly as possible. Addition of surfactants in this case may not be necessary, and may even have detrimental consequences, as observed in this work for myoglobin. If freezing is performed in larger vessels, fast freezing may also improve the homogeneity of solutes distribution throughout the geometry of the cake.[66] In all cases, addition of cryoprotectants, such as the disaccharides sucrose and trehalose, would be beneficial.[64]

If the protein formulation has to be stored in the frozen state, storage should be performed below the T_g' of the matrix to avoid processes triggered by mobility above T_g' (e.g., protein unfolding and aggregation or solutes crystallization).[66] Considering what is reported in the literature about the effect of thawing on protein stability[27], a fast thawing rate may be beneficial for both bulk-denaturing and surface-denaturing proteins, as it minimizes both process duration and the risks of recrystallization. However, the effect of thawing was not addressed in the present work, and additional investigation is needed on this point. If the objective is to store the protein in a freeze-dried state, proteins with high bulk stability should be frozen at a slow cooling rate, which also results in the best process efficiency (Figure 10). However, if the protein being dried is extremely prone to cold denaturation, a high cooling rate would preserve biological activity the most. If the increase in drying time resulting from the fast cooling rate is not economically viable, a proper choice of the formulation (i.e., addition of a sufficient amount of effective cryoprotectants) may still make it possible to obtain an acceptable protein recovery with a slower cooling rate. The model herein presented is just a first attempt to describe the freezing behavior of proteins, and the hope is that it will stimulate further studies in this direction.

CONCLUSIONS

Using the proposed approach, based on mathematical modeling and the use of the design space, two opposite situations have been studied. If the protein is more stable in the bulk solution than at the ice interface, the freezing process should be designed so as to result in a small ice-water surface area. This would also be beneficial for the primary drying step of freeze drying, which could be completed in a shorter

time and with reduced risk of product collapse. On the contrary, a high cooling rate, resulting in fast immobilization of the protein in a glassy matrix, should be preferred if the protein being frozen is poorly stable in solution. This result, suggested by *in silico* modelling, is confirmed by experimental results for lactate dehydrogenase and myoglobin as model proteins. Identification of these two opposite behaviors also makes it possible to improve our understanding of protein stability, by separating the effects of surface-driven denaturation and cold unfolding. In many cases these two mechanisms are closely interrelated, making it difficult to distinguish, for instance, the effect of surfactants on the bulk behavior of a protein. Here we have shown that surfactants are not only involved in surface-driven phenomena, but may also have an effect on protein conformation in the bulk. Specifically, Tween 80 was found to promote myoglobin unfolding in the bulk, while stabilizing agents such as sucrose, trehalose, and to a lesser extent also mannitol, counteracted this denaturing effect. Overall, the data reported in this work suggest that the freezing process is crucial for protein stability. These considerations may help people involved in the preservation of proteins and other biomolecules to improve the final recovery of therapeutic activity.

ACKNOWLEDGEMENTS

The authors would like to thank Francesca Susa, Tania Limongi and Valentina Cauda for their help with experimental analyses. Camilla Moino is acknowledged for her help with those runs involving the VISF freezing method.

REFERENCES

[1] Moorkens E, Meuwissen N, Huys I, Declerck P, Vulto AG, Simoens S. The market of biopharmaceutical medicines: A snapshot of a diverse industrial landscape. Front Pharmacol 2017;8:314.

[2] Wang W, Roberts CJ. Aggregation of therapeutic proteins. Hoboken, New Jersey: John Wiley & Sons, Inc.; 2010.

[3] Privalov PL. Cold denaturation of proteins. Crit Rev Biochem Mol Biol 1990;25(4):281-305.

[4] Franks F. Protein destailization at low temperatures. Adv Protein Chem 1995;46:105-139.

[5] Graziano G, Catanzano F, Riccio A, Barone G. A reassessment of the molecular origin of cold denaturation. J Biochem 1997;122(2):395-401.

[6] Lopez CF, Darst RK, Rossky PJ. Mechanistic elements of protein cold denaturation. J Phys Chem B 2008;112(19):5961-5967.

[7] Matysiak S, Debenedetti PG, Rossky PJ. Role of hydrophobic hydration in protein stability: A 3d water-explicit protein model exhibiting cold and heat denaturation. J Phys Chem B 2012;116(28):8095-8104.

[8] Strambini GB, Gabellieri E. Proteins in frozen solutions: Evidence of ice-induced partial unfolding. Biophys J 1996;70(2):971-976.

[9] Al-Hussein A, Gieseler H. The effect of mannitol crystallization in mannitol-sucrose systems on LDH stability during freeze-drying. J Pharm Sci 2012;101(7):2534-2544.

[10] Pikal MJ. Mechanisms of protein stabilization during freeze-drying storage: The relative importance of thermodynamic stabilization and glassy state relaxation dynamics. In: Rey L, May JC, eds. *Freeze-Drying/Lyophilization of Pharmaceutical and Biological Products*, London: Informa Healthcare; 2010;198-232.

[11] van den Berg L, Rose D. The effect of freezing on the pH and composition of sodium and potassium solutions: The reciprocal system KH_2PO_4-Na_2HPO_4-H_2O. Arch Biochem Biophys 1959;81(2):319-329.

[12] Anchordoquy TJ, Carpenter JF. Polymers protect lactate dehydrogenase during freeze-drying by inhibiting dissociation in the frozen state. Arch Biochem Biophys 1996;332(2):231-238.

[13] Gómez G, Pikal MJ, Rodríguez-Hornedo N. Effect of initial buffer composition on pH changes during far-from-equilibrium freezing of sodium phosphate buffer solutions. Pharm Res 2001;18(1):90-97.

[14] Murase N, Franks F. Salt precipitation during the freeze-concentration of phosphate buffer solutions. Biophys. Chem. 1989;34(3):293-300.

[15] Heller MC, Carpenter JF, Randolph TW. Manipulation of lyophilization induced phase separation:

Implications for pharmaceutical proteins. Biotechnol Prog 1997;13(5):590-596.

[16] Liu W, Wang DQ, Nail SL. Freeze-drying of proteins from a sucrose-glycine excipient system: Effect of formulation composition on the initial recovery of protein activity. AAPS PharmSciTech 2005;6(2):150-157.

[17] Hottot A, Vessot S, Andrieu J. Freeze-drying of pharmaceuticals in vials: Influence of freezing protocol and sample configuration on ice morphology and freeze-dried cake texture. Chem Eng Process 2007;46(7):666-674.

[18] Kasper JC, Friess WF. The freezing step in lyophilization: Physico-chemical fundamentals, freezing methods and consequences on process performance and quality attributes of biopharmaceuticals. Eur J Pharm Biopharm 2011;78(2):248-263.

[19] Franks F. Solid aqueous solutions. Pure Appl Chem 1993;65(12):2527-2537.

[20] Chang BS, Randall CS. Use of subambient thermal analysis to optimize protein lyophilization. Cryobiology 1992;29(5):632-656.

[21] Hsu CC, Walsh AJ, Nguyen HM, Overcashier DE, Koning-Bastiaan H, Bailey RC, Nail SL. Design and application of a low-temperature Peltier-cooling microscope stage. Chem Eng Process 1996;85(1):70-74.

[22] Kim AI, Akers MJ, Nail SL. The physical state of mannitol after freeze-drying: Effect of mannitol concentration, freezing rate, and a noncrystallizing cosolute. J Pharm Sci 1998;87(8):931-935.

[23] Akers MJ, Milton N, Byrn SR, Nail SL. Glycine crystallization during freezing: The effects of salt form, pH, and ionic strength. Pharm Res 1995;12(10):1457-1461.

[24] Cao W, Xie Y, Krishnan S, Lin H, Ricci M. Influence of process conditions on the crystallization and transition of metastable mannitol forms in protein formulations during lyophilization. Pharm Res 2013;30(1):131-139.

[25] Peters BH, Staels L, Rantanen J, Molnar F, De Beer T, Lehto VP, Ketolainen J. Effects of cooling rate in microscale and pilot scale freeze-drying - Variations in excipient polymorphs and protein secondary structure. Eur J Pharm Sci 2016;95:72-81

[26] Searles J, Carpenter J, Randolph T. The ice nucleation temperature determines the primary drying rate of lyophilization for samples frozen on a temperature-controlled shelf. J Pharm Sci, 2001;90(7):860-871.

[27] Cao E, Chen Y, Cui Z, Foster PR. Effect of freezing and thawing rates on denaturation of proteins in aqueous solutions. Biotechnol Bioeng 2003;82(6):684-690.

[28] Oddone I, Barresi AA, Pisano R. Influence of controlled ice nucleation on the freeze-drying of pharmaceutical products: The secondary drying step. Int J Pharm 2017;524(1-2):134-140.

[29] US Food and Drug Administration, Department of health and human services, Pharmaceutical cGMPs for the 21st century: A risk-based approach, 2002.

[30] Yu LX. Pharmaceutical quality by design: product and process development, understanding, and control. Pharm Res 2008;25(4):781-791.

[31] Yu LX, Amidon G, Khan MA, Hoag SW, Polli J, Raju GK, Woodcock J. Understanding pharmaceutical quality by design. AAPS J 2014;16(4):771-783.

[32] Singh SK, Kolhe P, Wang W, Nema S. Large-scale freezing of biologics: A practitioner's review, part 1-fundamental aspects. BioProcess Int. 2009;7(9):32-44.

[33] Zwanzig R. Two-state models of protein folding kinetics. Proc Natl Acad Sci USA 1997;94(1):148-150.

[34] Creighton TE. Toward a better understanding of protein folding pathways. Proc Natl Acad Sci USA 1988;85(14):5082-5086.

[35] Scalley ML, Baker D. Protein folding kinetics exhibit an Arrhenius temperature dependence when corrected for the temperature dependence of protein stability. Proc Natl Acad Sci USA 1997;94(20):10636-10640.

[36] Plaxco KW, Baker D. Limited internal friction in the rate-limiting step of a two-state protein folding reaction. Proc Natl Acad Sci USA 1998;95(23):13591-13596.

[37] Haas E, Katchalski-Katzir E, Steinberg IZ. Brownian motion of the ends of oligopeptide chains in solution as estimated by energy transfer between the chain ends. Biopolymers 1978;17(1):11-31.

[38] Ansari A, Jones CM, Henry ER, Hofrichter J, Eaton WA. The role of solvent viscosity in the dynamics of protein conformational changes. Science 1992;256(5065):1796-1798.

[39] Kleinert T, Doster W, Leyser H, Petry W, Schwarz V, Settles M. Solvent composition and viscosity effects on the kinetics of CO binding to horse myoglobin. Biochemistry 1998;37(2):717-733.

[40] Arsiccio A, Barresi AA, Pisano R. Prediction of ice crystal size distribution after freezing of pharmaceutical solutions. Cryst Growth Des 2017;17(9):4573-4581.

[41] Arsiccio A, Barresi AA, De Beer T, Oddone I, Van Bockstal P-J, Pisano R. Vacuum induced surface freezing as an effective method for improved inter- and intra-vial product homogeneity. Eur J Pharm Biopharm 2018;128:210-219.

[42] Arsiccio A, Pisano R. Application of the Quality by Design approach to the freezing step of freeze drying:

Building the design space. J Pharm Sci 2018;107(6):1586-1596.

[43] Young FE, Jones FT. Sucrose hydrates. The sucrose–water phase diagram. J Phys Chem 1949;53(9):1334-1350.

[44] Longinotti MP, Corti HR. Viscosity of concentrated sucrose and trehalose aqueous solutions including the supercooled regime. J Phys Chem Ref Data 2008;37(3):1503-1515.

[45] Arsiccio A, McCarty J, Pisano R, Shea J-E. Effect of surfactants on surface-induced denaturation of proteins: Evidence of an orientation-dependent mechanism. J Phys Chem B 2018;122(49): 11390-11399.

[46] Fissore D, Pisano R. Computer-aided framework for the design of freeze-drying cycles: optimization of the operating conditions of the primary drying stage. Processes 2015;3(2):406-421.

[47] Oddone I, Pisano R, Bullich R, Stewart P. Vacuum-induced nucleation as a method for freeze-drying cycle optimization. Ind Eng Chem Res 2014;53(47):18236-18244.

[48] Oddone I, Van Bockstal P-J, De Beer T, Pisano R. Impact of vacuum-induced surface freezing on inter- and intra-vial heterogeneity. Eur J Pharm Biopharm 2016;103:167-178.

[49] Anderson AB, Robertson CR. Absorption spectra indicate conformational alteration of myoglobin adsorbed on polydimethylsiloxane. Biophys J 1995;68(5):2091-2097.

[50] Privalov PL. Thermodynamics of protein folding. J Chem Thermodyn 1997;29:447-474.

[51] Hatley RHM, Franks F. The cold-induced denaturation of lactate dehydrogenase at sub-zero temperatures in the absence of perturbants. FEBS Lett 1989;257(1):171-173.

[52] Pisano R. Alternative methods of controlling nucleation in freeze drying. In: Ward K, Matejtschuk P, eds. *Lyophilization of Pharmaceuticals and Biologicals. Methods in Pharmacology and Toxicology*, New York, NY: Humana Press;2019:79-111.

[53] Randolph TW, Jones LS. Surfactant-protein interactions. In: Carpenter JF, Manning MC, eds. *Rational Design of Stable Protein Formulations*. Boston, MA: Springer;2002:159-175.

[54] Lee HJ, McAuley A, Schilke KF, McGuire J. Molecular origins of surfactant-mediated stabilization of protein drugs. Adv Drug Deliv Rev 2011;63(13):1160-1171.

[55] Bhatnagar BS, Pikal MJ, Robin HB. Study of the individual contributions of ice formation and freeze-concentration on isothermal stability of lactate dehydrogenase during freezing. J Pharm Sci 2008;97(2):798-814.

[56] Chang BS, Kendrick BS, Carpenter JF. Surface-induced denaturation of proteins during freezing and its

inhibition by surfactants. J Pharm Sci 1996;85(12):1325-1330.

[57] Shosheva A, Miteva M, Christova P, Atanasov B. pH-dependent stability of sperm whale myoglobin in water-guanidine hydrochloride solutions. Eur Biophys J 2003;31(8):617-625.

[58] Chou DK, Krishnamurthy R, Randolph TW, Carpenter JF, Manning MC. Effects of Tween 20® and Tween 80® on the stability of albutropin during agitation. J Pharm Sci 2005; 94(6):1368-1381.

[59] Bam NB, Cleland JL, Yang J, Manning MC, Carpenter JF, Kelley RF, Randolph TW. Tween protects recombinant human growth hormone against agitation-induced damage via hydrophobic interactions. J Pharm Sci 1998;87(12):1554-1559.

[60] Deechongkit S, Wen J, Narhi LO, Jiang Y, Park SS, Kim J, Kerwin BA. Physical and biophysical effects of polysorbate 20 and 80 on darbepoetin alfa. J Pharm Sci 2009;98(9):3200-3217.

[61] Arsiccio A, Pisano R. Surfactants as stabilizers for biopharmaceuticals: An insight into the molecular mechanisms for inhibition of protein aggregation. Eur J Pharm Biopharm 2018;128:98-106.

[62] Bam NB, Cleland JL, Randolph TW. Molten globule intermediate of recombinant human growth hormone: Stabilization with surfactants. Biotechnol Prog 1996;12(6):801-809.

[63] Jones LS, Randolph TW, Kohnert U, Papadimitriou A, Winter G, Hagmann ML, Manning MC, Carpenter JF. The effects of Tween 20 and sucrose on the stability of anti-L-selectin during lyophilization and reconstitution. J Pharm Sci 2001;90(10):1466-1477.

[64] Tang XC, Pikal MJ. The effect of stabilizers and denaturants on the cold denaturation temperatures of proteins and implications for freeze-drying. Pharm Res 2005;22(7):1167-1175.

[65] Webb SD, Webb JN, Hughes TG, Sesin DF, Kincaid AC. Freezing bulk-scale biopharmaceuticals using common techniques - and the magnitude of freeze-concentration. BioPharm 2002;15(5):22–34.

[66] Miller MA, Rodrigues MA, Glass MA, Singh SK, Johnston KP, Maynard JA. Frozen-state storage stability of a monoclonal antibody: Aggregation is impacted by freezing rate and solute distribution. J. Pharm. Sci. 2013;12(4):1194-1208.

LIST OF TABLES

Table 1. Details of the simulations performed

	ΔH_0, kJ mol^{-1}	m, kJ mol^{-1} M^{-1}	A, s^{-1}	Reversible
1	80	4	2□10^2	yes
2	60	1	2□10^2	yes
3	100	4	2□10^1	no
4	80	4	2□10^2	no

LIST OF FIGURES

Figure 6: Percentage of LDH recovery after shelf-ramped freezing at 1 K min^{-1} (grey bars) or quench freezing (blue bars), both in presence (plain bars) and absence (dashed bars) of Tween 80, as measured from (a) the increase in absorbance at 450 nm due to the enzymatic reduction of NAD to NADH or (b) the increase in OD at 500 nm. For panel (a) data have been normalized relative to the formulation before freeze-thaw. For panel (b) data have been normalized relative to the buffer only formulation after shelf-ramped freezing (in absence of surfactant).

Figure 7: Percentage of myoglobin recovery after 1 (dashed bars) and 3 (colored bars) freeze-thaw cycles performed using the VISF controlled nucleation technique (black bars), shelf-ramped freezing at 1 K min^{-1} (blue bars) or quench freezing in liquid nitrogen (orange bars), as measured from the decrease in OD at 280 nm (a) or 410 nm (b). Data have been normalized relative to the formulation before freeze-thaw.

Figure 8: Percentage of myoglobin recovery after one freeze-thaw cycle, as measured from the decrease in OD at 410 nm. Different formulations were considered, including 5% mannitol, 5% sucrose, 5% trehalose, or citrate buffer only, both in absence (dashed bars) and presence (grey bars) of Tween 80. Data have been normalized relative to the formulation before freeze-thaw.

Figure 9: Protein recovery as function of time, in non-frozen samples, during storage at 268 K. Both 0.1 mg/ml Mb in sodium citrate buffer at pH 3.7 (solid lines) and 0.1 mg/ml LDH in sodium citrate buffer at pH 6.5 (dashed lines) were considered, either in presence (red line, square symbol) or absence (black line, circle symbol) of 0.01 % w/v Tween 80.

Figure 10: Design space showing the primary drying time t_d and the maximum temperature T_{max} reached within the product as function of nucleation temperature and cooling rate used during the freezing phase. A fluid temperature and chamber pressure of 253 K and 10 Pa, respectively, have been considered for simulations of the primary drying step.

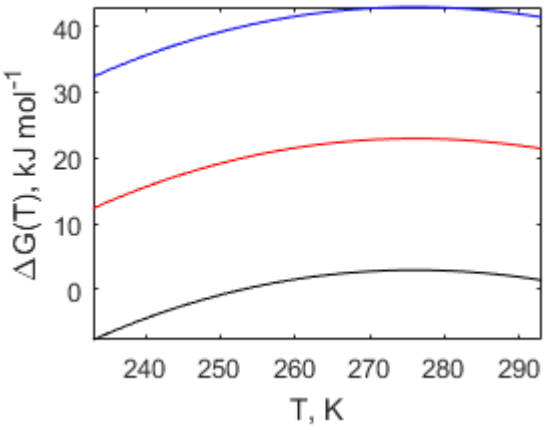

Figure 1

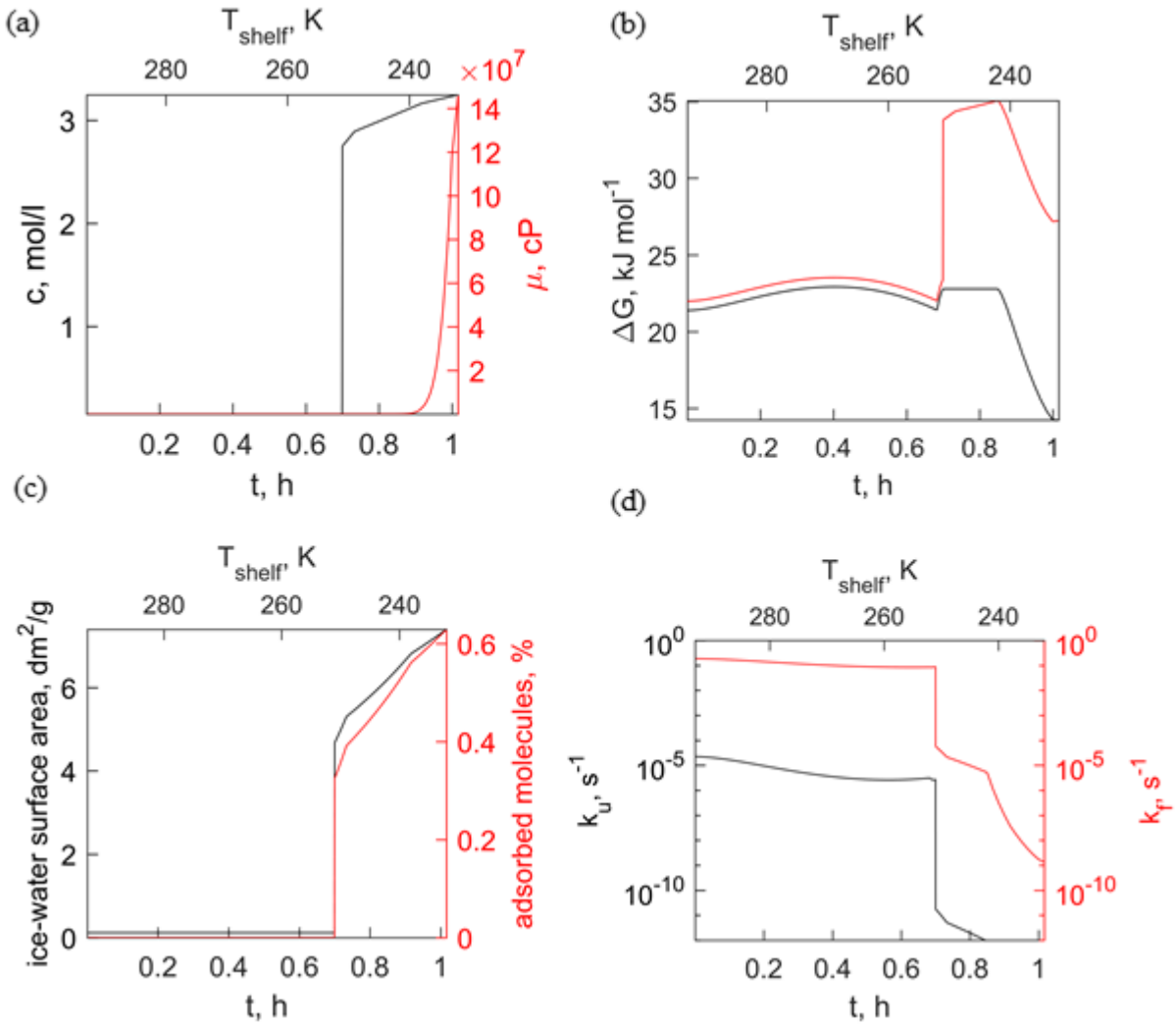
(a)
T shelf, K
280
260
240
×10^7
c, mol/l
μ, cP
t, h
(b)
T shelf, K
ΔG, kJ mol^-1
t, h
(c)
T shelf, K
ice-water surface area, dm^2/g
adsorbed molecules, %
t, h
(d)
T shelf, K
k_u, s^-1
k_f, s^-1
t, h

Figure 2

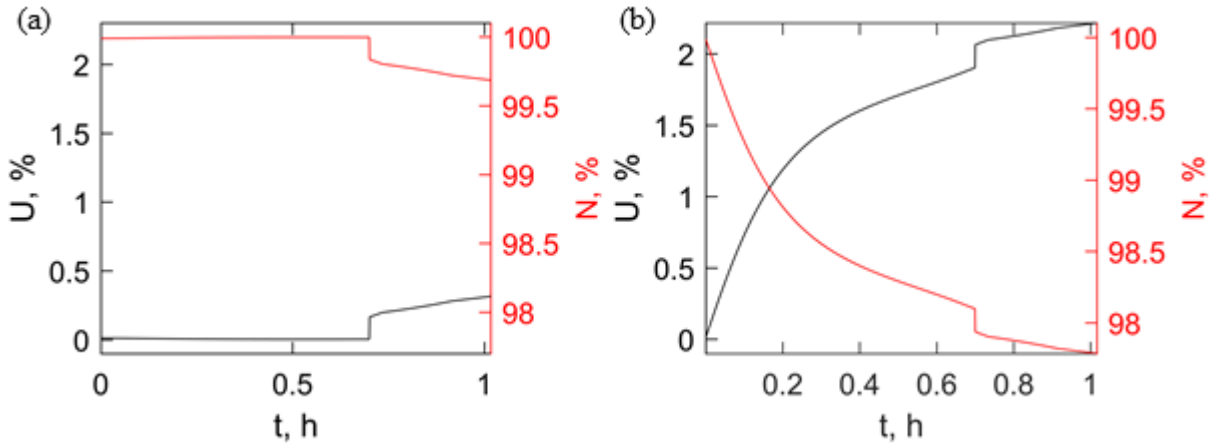
(a)
U, %
N, %
t, h
0
0.5
1
1.5
2
98
98.5
99
99.5
100
(b)
U, %
N, %
t, h
0
0.2
0.4
0.6
0.8
1
0.5
1
1.5
2
98
98.5
99
99.5
100

Figure 3

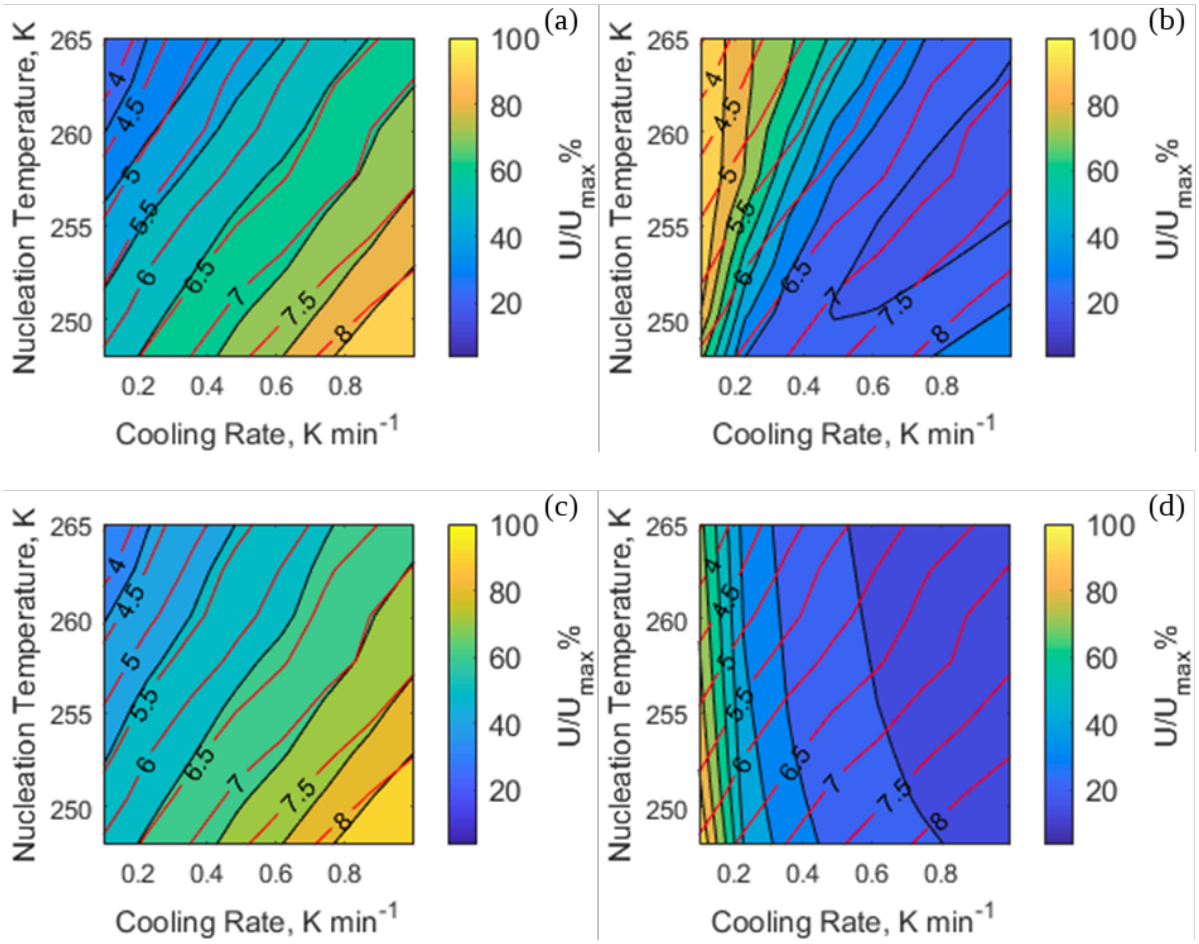
(a)
(b)
(c)
(d)
Nucleation Temperature, K
265
260
255
250
0.2
0.4
0.6
0.8
Cooling Rate, K min-1
4
4.5
5
5.5
6
6.5
7
7.5
8
100
80
60
40
20
U/Umax %

Figure 4

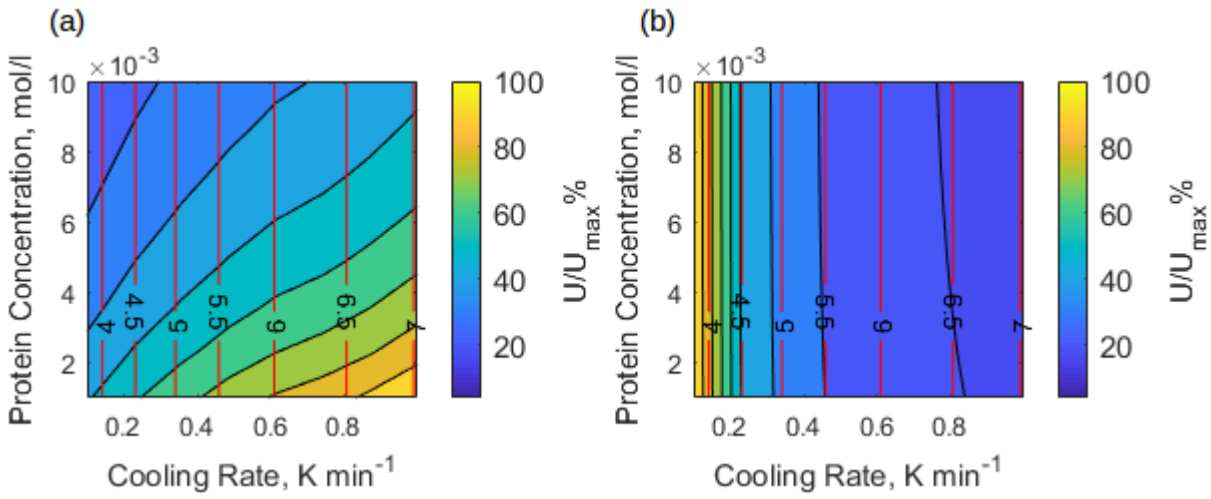
(a)
(b)
Protein Concentration, mol/l
×10^-3
10
8
6
4
2
0.2
0.4
0.6
0.8
Cooling Rate, K min^-1
4
4.5
5
5.5
6
6.5
7
100
80
60
40
20
U/U_max %

Figure 5

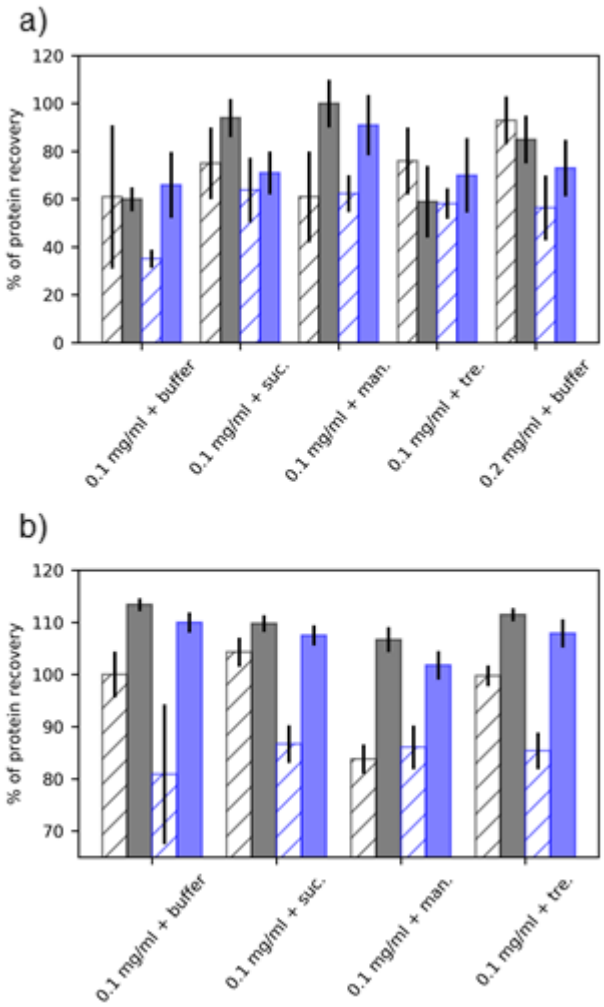
a)
% of protein recovery
120
100
80
60
40
20
0
0.1 mg/ml + buffer
0.1 mg/ml + suc.
0.1 mg/ml + man.
0.1 mg/ml + tre.
0.2 mg/ml + buffer
b)
% of protein recovery
120
110
100
90
80
70
0.1 mg/ml + buffer
0.1 mg/ml + suc.
0.1 mg/ml + man.
0.1 mg/ml + tre.

Figure 6

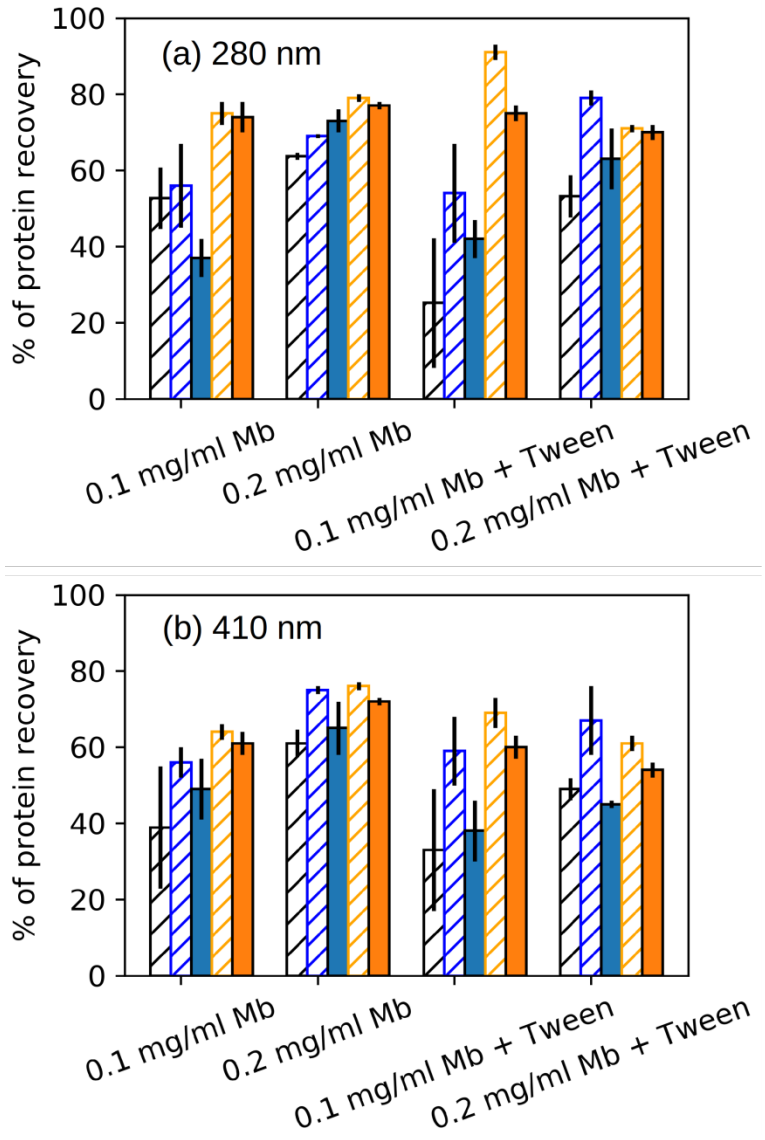
(a) 280 nm
% of protein recovery
100
80
60
40
20
0
0.1 mg/ml Mb
0.2 mg/ml Mb
0.1 mg/ml Mb + Tween
0.2 mg/ml Mb + Tween
(b) 410 nm
% of protein recovery
100
80
60
40
20
0
0.1 mg/ml Mb
0.2 mg/ml Mb
0.1 mg/ml Mb + Tween
0.2 mg/ml Mb + Tween

Figure 7

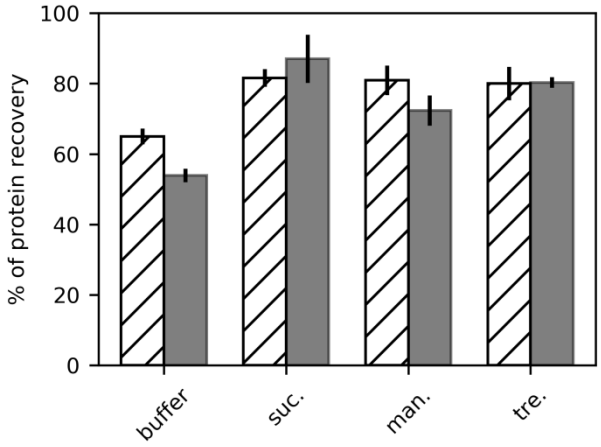

Figure 8

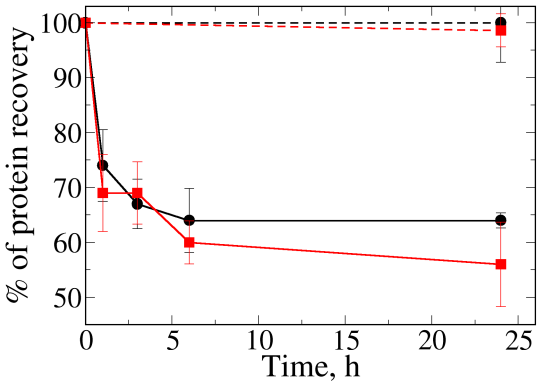

Figure 9

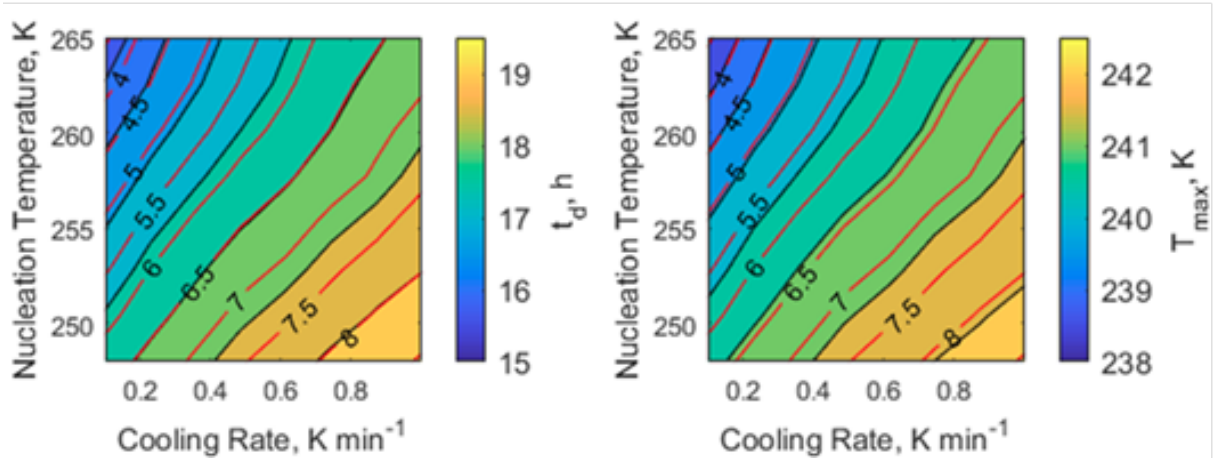
Nucleation Temperature, K
265
260
255
250
4
4.5
5
5.5
6
6.5
7
7.5
8
0.2
0.4
0.6
0.8
Cooling Rate, K min-1
19
18
17
16
15
td, h
Nucleation Temperature, K
265
260
255
250
4
4.5
5
5.5
6
6.5
7
7.5
8
0.2
0.4
0.6
0.8
Cooling Rate, K min-1
242
241
240
239
238
Tmax, K

Figure 10